



# Drought severity modeling of upper Bhima river basin, western India, using GIS–AHP tools for effective mitigation and resource management

Nayan D. Zagade<sup>1</sup> · Bhavana N. Umrikar<sup>2</sup> 

Received: 8 April 2020 / Accepted: 26 September 2020  
© Springer Nature B.V. 2020

## Abstract

The combination of geographic information system (GIS) and analytic hierarchy process (AHP) performs the drought vulnerability assessment of larger areas efficiently. The drought intensity and types are locale specific, and hence the spatial distribution helps in formulating the strategies to combat this natural hazard. With this view, the drought-prone and vulnerable areas in upper Bhima river basin from western India were delineated considering the ten associated parameters, viz. NDVI, rainfall, slope, vadose zone, soil depth, LULC, water harvesting structures, geomorphology, drainage density and groundwater level fluctuation. AHP was employed composing the pairwise and normalized pairwise comparison matrix to obtain the relative weight of each parameter. The cumulative effect of influencing parameters was considered to generate the drought zonation map of the region in the GIS environment. The resultant map depicts that about 24% area falls under the severe drought and about 31% area in moderate drought zones. This drought severity mapping could be helpful in preparedness and providing water scarcity relief measures to the affected villages in the region.

**Keywords** Drought severity · AHP · GIS · Basaltic terrain · Western India

## 1 Introduction

Drought is a slow approaching hazard that manifests through diminished springs, stream flow, base flow, crop wilting, soil moisture reduction, dry wells, etc. Mostly, drought is a climate-driven phenomenon that has been studied time to time with different perspectives. However, the common goal has been to understand the driving forces and suggest drought management strategies. Since the phenomenon is recurring and having nonstructural

---

**Electronic supplementary material** The online version of this article (<https://doi.org/10.1007/s11069-020-04350-9>) contains supplementary material, which is available to authorized users.

---

✉ Bhavana N. Umrikar  
bnumrikar@gmail.com

<sup>1</sup> Department of Geography, Savitribai Phule Pune University, Pune, India

<sup>2</sup> Department of Geology, Savitribai Phule Pune University, Pune, India

impacts, diligent efforts are needed to address drought-related issues through immediate and long-term measures. Besides, the quantification of drought is very difficult because of the sector-specific scale (hydrological, meteorological, agricultural and socioeconomic). Moreover, the risk, severity and duration of drought vary from place to place with various outlooks worldwide and thus do not have any unanimously accepted definition (Van Loon et al. 2016; Yihdego et al. 2019). Generally, a deficit in precipitation from an expected mean within a time frame can be broadly identified as drought (Svoboda et al. 2002; Sheffield and Wood 2012; Eslamian 2014; Kamali et al. 2017; Yihdego 2017).

As the drought hazard footprints are complex and significant, the prediction and mitigation require consideration of interdisciplinary factors. Various studies have focused on developing hydrometeorological drought indices for monitoring and evaluation (Palmer 1965, 1968; McKee et al. 1993; Vicente-Serrano et al. 2010; Golian et al. 2015; Thomas et al. 2016; Murthy et al. 2016; Vijaya Kumar et al. 2019). Apart from this, a growing trend of using RS-GIS and multi-criteria decision tools has been witnessed for mapping various natural hazards in recent decades (Pogarčić et al. 2008; Prathumchai et al. 2001; Chen et al. 2011; Pandey et al. 2012; Stefanidis and Stathis 2013; Palchaudhuri and Biswas 2016; Zagade et al. 2018). GIS helps in figuring out various data sets necessary for disaster monitoring and also has the potential to integrate and analyze various types of data sets for larger areas (Chopra 2006; Tao et al. 2011). The availability of high-frequency remotely sensed data has helped in real-time monitoring and forecasting of natural hazards (Han et al. 2010). Decision-making by multi-criteria analysis is in vogue such as analytical hierarchical process (AHP) that facilitates a multi-criteria comparison matrix (Saaty 1980) and also helps in removing the biases in judgment of weightage assigned to factors contributing to drought.

Drought is a major concern in the upper Bhima catchment area of western India (Gaur et al. 2007). Severe and prolonged droughts experienced in the last few decades have drawn the attention of developers, planners and researchers to this region. With this background, the present study has been carried out to develop a multi-parameter model revealing the spatial spread of drought in the hard rock terrain of Bhima River catchment, Maharashtra, India, by deploying integrated techniques of RS-GIS and analytical hierarchy process (AHP). The mapping has been carried out with a range of variables and aggregated measures of drought to identify vulnerable areas by integrating traditional hydrogeological field surveyed data, remotely sensed data and ancillary data for effective mitigation planning. Until now, no such drought susceptibility studies have been reported from this region; therefore, it would be the pioneer work that is crucial for preparedness of sectoral drought.

## 2 Study area

The study area includes four sub-watersheds, namely BM-7, BM-17, BM-33 and BM-34, of upper Bhima river basin with a areal spread of 1778.16 sq. km representing Deccan Basaltic Province. It is bounded by 73°50'41" to 74°40'07" E longitude and 18°29'11" to 19°10'23" N latitude falling in Survey of India toposheet numbers 47 J/5, J/6, J/9 and J/10. The area is situated on the border of Pune and Ahmednagar districts covering a part of Ambegaon, Junnar, Shirur talukas of Pune District and Shrigonda and Parner talukas of Ahmednagar District which is in rain shadow zone of Western Ghats (Fig. 1).

Ghod, the tributary of Bhima river, is the mainstream in the region, while Meena and Kukadi are the tributaries of Ghod river. The area receives monsoonal rain that begins in

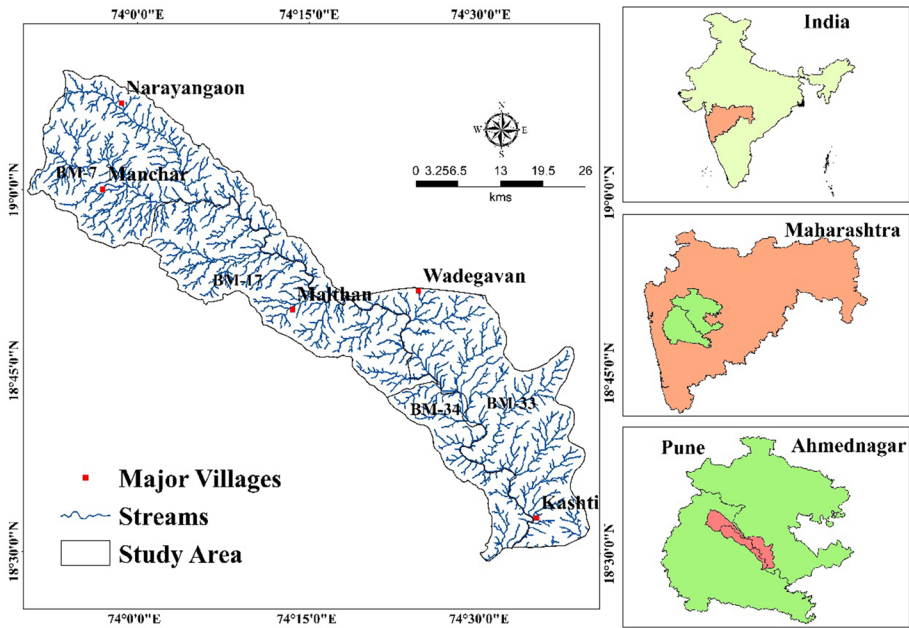


**Fig. 1** Location map of the study area

the month of June and lasts till the end of September with an annual average of 497 mm. The return monsoon showers are received in the month of October and November. The study area experiences hot tropical climate with temperature raising up to 39 °C in summer months of April and May. The average yearly maximum temperature is about 32 °C and minimum 21 °C. Agriculture is the major land use in the region, and mostly rain-fed crops like millets, soybean, corn, wheat, etc., are popular. Besides, sugarcane is mostly observed in the central and lower part of the watershed. Groundwater is the prime source of domestic and irrigation, explored from large diameter dug wells tapping amygdaloidal, vesicular, fractured and jointed shallow basaltic aquifers. Due to the absence of primary porosity in basaltic rocks, the availability and movement of groundwater is restricted to the degree of weathering, jointing, fracturing and connectivity of vesicles in basalts. Moreover, the groundwater in the phreatic state joins the surface water in the form of base flow. As a result, the area faces drought, particularly the villages in hilly regions, very frequently.

### 3 Data sources and methodology

To determine the drought-prone zones in the upper Bhima area, geospatial techniques integrated with multi-criteria decision (AHP) method have been used considering the factors that are influencing drought vulnerability, namely NDVI, rainfall, slope, vadose zone, soil depth, LULC, water harvesting structures, geomorphology, drainage density and groundwater level fluctuation. The details of various data sources, data preparation in GIS environment and application of AHP method are discussed below:

### 3.1 Generation of thematic layers

Rainfall variability with prolonged dry spells, hike in total dry days and light precipitation events are related to drought (Sun et al. 2007; Dash et al. 2009; Liu et al. 2009; Mishra and Liu 2014; Pathak and Dodamani 2020); hence, daily rainfall data have been used to understand drought characteristics and the intensity in the area. The high-resolution (0.250 \* 0.250 grid) precipitation data were downloaded from IMD Web site and converted to shape file using Open Grade Software. The sum of daily rainfall was performed using raster calculator, and the rainfall data from 13 rain gauge stations available on the Web site (<https://krishi.maharashtra.gov.in>) of Department of Agriculture were merged to generate annual rainfall distribution map by IDW interpolation method for the drought assessment year (2018).

Normalized difference vegetation index (NDVI) is used for monitoring vegetation cover, identification of different crops, the health of plants and growth pattern of agriculture. The intensity and density of green cover are computed using the vegetative reflectance in red and near-infrared wavelengths (Eq. 1).

$$NDVI = \frac{\rho_{NIR} - \rho_{Red}}{\rho_{NIR} + \rho_{Red}} \quad (1)$$

where  $\rho_{Red}$  and  $\rho_{NIR}$  are the reflectance for Landsat band 4 (630–680 nm) and band 5 (845–885 nm), respectively.

Landsat 8 Operational Land Imager (OLI)/Thermal Infrared Sensor (TIRS) C1 Level 1 was downloaded from USGS Earth Explorer (December 2018) to generate the NDVI and LU/LC layers of the area. Land slope is one of the decisive factors for runoff–recharge ratio and also has an influence on groundwater availability. Slope layer has been generated using Cartosat Digital Elevation Model (DEM) downloaded from BHUVAN Web site, with 30 m resolution applying spatial analyst tool. The stream flow lines were extracted from DEM using hydro-tool, and a drainage density map was created by applying a line density algorithm in GIS.

The thickness of the vadose zone was determined during hydrogeological field surveys and dug well inventory conducted in the study area. Soil depth and geomorphology maps were prepared by referring to the regional resource map of National Bureau of Soil Survey (NBSS) and National Atlas and Thematic Mapping Organization (NATMO), respectively. Landsat imagery was processed to understand the land use/land cover (LU/LC) pattern in the area. Image processing and a supervised classification tool with maximum likelihood algorithm helped in performing the analysis. Hills, agriculture, barren land, fallow land, settlement, vegetation, and water body are the major classes defined to generate LU/LC theme. Existing surface water harvesting structures were manually digitized from Google Earth images and density of structures was computed using point density tool in GIS. Depth to the groundwater level data for pre- and post-monsoon seasons were procured for the hydrogeological year 2018–2019, from the state groundwater organization for generating groundwater level fluctuation map. The flowchart of methodology adopted during this study is shown in Fig. 2. The list of tanker-fed villages falling in the study area was procured (2018–2019) from Groundwater Surveys and Development Agency, Pune (GSDA), to validate the drought zonation model.

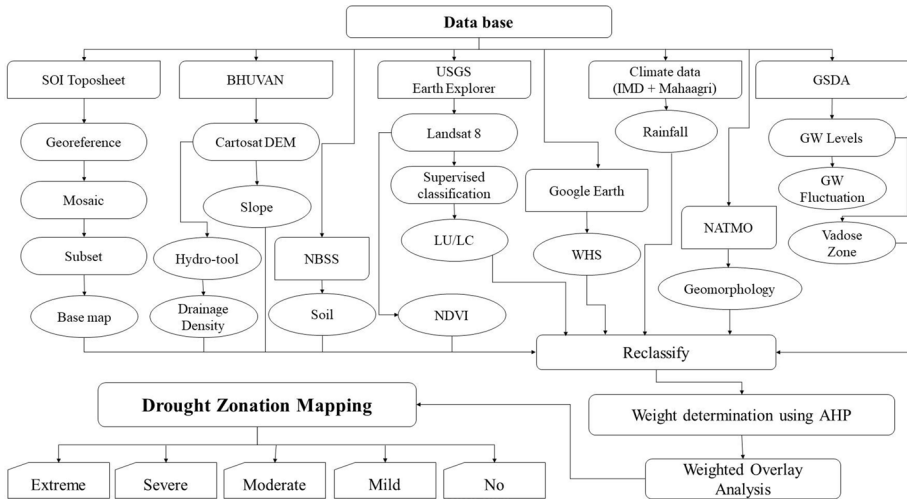


Fig. 2 Methodology chart

### 3.2 AHP model

AHP is a popular tool among the researchers that is capable of comparing the factors as per their relative importance over one another to determine the priorities. Therefore, AHP was employed to decipher the drought-prone zones of the selected area. The assignment of weights to the influencing factors in hierarchical dominance framework has been carried out by following the steps as discussed below:

#### 3.2.1 Generation of a hierarchy structure

The process for spatial multi-criteria decision problems involves the development of a value structure of evaluation criteria wherein the objectives and the respective alternative follow a hierarchy relation (Malczewski 1999). The hierarchy structure has been designed for the various influential factors, namely NDVI, rainfall, slope, vadose zone, soil depth, LULC, water harvesting structures, geomorphology, drainage density and groundwater level fluctuation. The highest value is conferred to criteria of most significance and lowest to the least important.

#### 3.2.2 Pairwise comparison matrix

The pairwise comparison matrix (PWCM) rates the factors according to their relation (strong or weak) with other factors and the degree of influence on drought severity. For the generation of PWCM of dimensions  $n \times n$  (number of criteria compared), a scale of values ranging from 9 to 1/9, developed by Saaty (1977), was referred (Table 1).

**Table 1** Comparison matrix scale (Saaty 1977)

Comparison for parameters (1 to 9 scale)	
Intensity of importance	Definition
1.00	Equal
3.00	Moderate
5.00	Strong
7.00	Very strong
9.00	Extreme
2, 4, 6, 8	For compromises between the above

The highest rating, i.e., 9, hints the row factor to be more dominating over the column factor and vice versa with the lowest rating value 1/9. The expertise inputs were taken into consideration while deciding the ranks of influential factors.

### 3.2.3 Consistency ratio (CR)

Consistency ratio is a single numerical index that verifies the consistency of PWCM (Saaty, 1980); if CR is less than 10% then the hierarchical structure and ranks are accepted. Saaty and Vargas (1991) recommended a revision of the preference matrix by the expert's knowledge and experience, if the CR value is higher than 1. Consistency ratio is computed by using Eq. 2:

$$CR = \frac{CI}{RI} \quad (2)$$

where CI=consistency index for the set of judgments and RI=random index.

Equation 3 has been used to calculate the CI:

$$CI = \frac{\lambda_{\max} - n}{n - 1} \quad (3)$$

Where  $\lambda_{\max}$  = greatest eigenvalue of preference matrix and  $n$  = order of matrix.

Eigenvalues are obtained by summing up the product of total weight and normalized weight of the evaluating criteria in the matrix. Further, the largest eigenvalue is considered as  $\lambda_{\max}$  to check the decision consistency of the PWCM.

RI values proposed by Saaty (1980) show the magnitude value for 10 criteria as 1.49 (Table 2).

## 4 Results and discussion

### 4.1 Thematic maps

#### 4.1.1 Normalized difference vegetation index (NDVI)

Normalized difference vegetation index has been derived to understand the intensity and density of vegetation cover in upper part of Bhima river basin. This index extends lagged

**Table 2** Values for RI (Saaty and Vargas 1991; where  $n$ =order of matrix)

No. of criteria (n)	1	2	3	4	5	6	7	8	9	10	11	12	13	14	15
RI	0.00	0.00	0.58	0.90	1.12	1.24	1.32	1.41	1.45	1.49	1.51	1.48	1.56	1.57	1.59

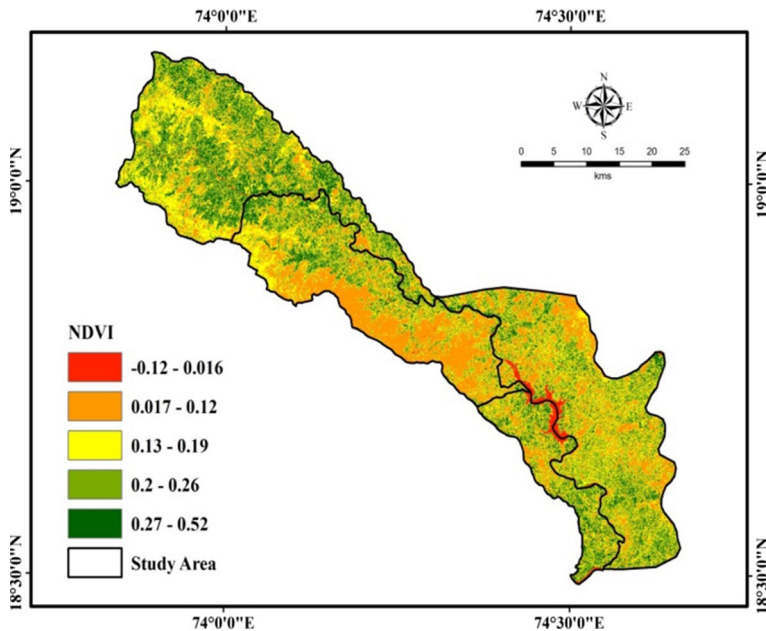


**Fig. 3** NDVI

response to drought and hence considered as an indirect factor in drought assessment. The NDVI value ranges from  $-0.12$  to  $0.52$  (Fig. 3). The map depicts that NDVI values between  $-0.1$  and  $0.12$  indicate the presence of water body, river or barren areas with exposed rocks occupying central part of the river basin. The index values varying from  $0.13$  to  $0.26$  depict the agricultural crops, fruit orchards and shrubs that are covering the southeastern part of the study area. Few patches that are observed toward northwest (in and around village Manchar) reveal undulating terrain, steep slopes covered with grass or shrubs. The high index values are indicative of more greenness in plants, dense vegetation canopy, forest or tree plantation occupying the northwest part as well as the mouth (village Kashti) of the basin. The lowest rank was assigned to high NDVI values as there is a minimum risk of drought and vice versa.

#### 4.1.2 Rainfall

The amount of rainfall, total rainy days, rainfall intensity and dry spells during rains have direct impact on drought severity. The dry spells between rainfall play very vital role in retaining moisture in soil zone and availability of water to various crops. Hence, it is the key factor in drought analysis. The normal average or above an average rainfall in a region experiences high surface runoff vis-a-vis high water levels in reservoirs, high cultivation of rain-fed crops and maximum aquifer saturation leading to elevated groundwater levels in dug wells. Rainwater is the prominent source of recharge in the study area. The rainfall distribution map was reclassified into five categories that depicts maximum rainfall of  $712.4$  mm and minimum  $259.72$  mm (Fig. 4). The high rainfall occurs in the NW area due to its proximity to Western Ghats causing orographic rains and gradually decreases toward

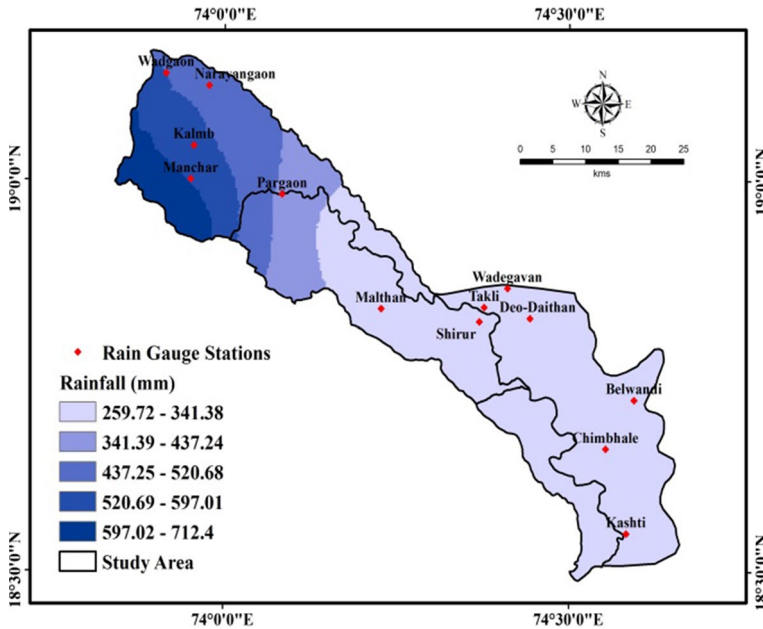


Fig. 4 Rainfall distribution

SE part. Majority of the area (783 sq. km) falls under very low rainfall category (Table 3). The highest ranks are assigned to the areas receiving less rainfall due to high drought vulnerability, and the lowest ranks to the areas showing maximum rainfall.

### 4.1.3 Slope

The land slope is a decisive factor in establishing the rainfall-to-runoff and rainfall-to-recharge ratio. The land having high degree slopes experiences short rainwater residence time; hence, there is a meager possibility of infiltration. The slope of land has been divided into five categories, viz. flat–gentle ( $0^{\circ}$ – $2.2^{\circ}$ ), low ( $2.3^{\circ}$ – $5.7^{\circ}$ ), moderate ( $5.8^{\circ}$ – $12^{\circ}$ ), high ( $13^{\circ}$ – $21^{\circ}$ ) and very high ( $22^{\circ}$ – $47^{\circ}$ ). Thus, with increasing degree of slope the water infiltration rate decreases resulting in more runoff (Khaleghi et al. 2017). Slopes also play a very significant role in setting land-use pattern altering the natural recharge rate. Majority of the area (86.82%, Table 3) falls under gentle to flat slope, i.e., plateau region (Fig. 5). The slope increases toward NW, especially in the peripheral hilly region where high runoff is generated; therefore, high ranks are assigned to very high slope category. Hence, the hamlets and small settlements situated in hilly areas of upper Bhima basin face the drinking water scarcity every year despite high rainfall.

### 4.1.4 Vadose zone

The vadose zone, also called as unsaturated zone or zone of aeration, consists of top soil layer, intermediate zone and capillary fringe belt above the water table. This zone characteristically represents the void/pore spaces that are partially filled with water. The thickness

**Table 3** Themes, AHP weights and area covered under each feature class

Sr. no	Theme	Classes	Rank	AHP weight	Area (sq km)	Area %
1	NDVI	−0.13–0.01	5	0.16743	409.633	23.0391
		0.01–0.12	4		822.155	46.2406
		0.13–0.19	3		433.864	24.4019
		0.2–0.27	2		104.987	5.9048
		0.28–0.54	1		7.354	0.4136
2	Rainfall	259.71–341.37	5	0.196972	783.01	44.0215
		341.38–437.24	4		380.287	21.3801
		437.25–520.67	3		182.25	10.2462
		520.68–597.01	2		276.796	15.5617
		597.02–712.40	1		156.357	8.7905
3	Slope	0–2.2	1	0.132175	1543.69	86.82
		2.3–5.7	2		143.703	8.0821
		5.8–12	3		43.388	2.442
		13–21	4		21.774	1.2246
		22–47	5		25.488	1.4335
4	Vadose zone	0.84–1.61	5	0.102781	888.417	49.9476
		1.61–2.57	4		455.6	25.6163
		2.57–3.42	3		378.531	21.2813
		3.42–5.59	2		45.144	2.538
		4.59–7.46	1		11.007	0.6188
5	Soil depth	Very shallow	5	0.105779	705.834	39.695
		Shallow	4		394.845	22.2053
		Moderately deep	3		41.934	2.3583
		Slightly deep	2		192.827	10.8441
		Deep	1		442.719	24.8976
6	LU/LC	Agriculture	2	0.063343	1080.801	59.7765
		Barren land and hills	5		500.510	28.1451
		Fallow land	3		58.070	3.2654
		Settlement	4		70.391	3.9582
		Waterbody and vegetation	1		68.551	3.8548
7	Density of WHS	Very high	1	0.109515	96.362	23.4157
		High	3		124.973	47.5202
		Moderate	2		165.142	14.9112
		Low	4		74.815	8.1442
		Very low	5		56.843	6.0087
8	Geomorphology	Denudational hills	5	0.034303	126.76	7.1356
		Plateau	4		1531.83	86.2296
		Alluvial plain	3		45.246	2.547
		Flood plain	2		3.112	0.1752
		Waterbody	1		69.505	3.9126

**Table 3** (continued)

Sr. no	Theme	Classes	Rank	AHP weight	Area (sq km)	Area %
9	Drainage density	Very high	5	0.040713	541.458	30.4635
		High	4		409.179	23.0213
		Moderate	3		417.947	23.5146
		Low	2		235.981	13.2768
		Very low	1		172.826	9.7236
10	Groundwater fluctuation	1.55–4.17	1	0.04699	8.155	0.4586
		4.18–5.61	2		316.736	17.8124
		5.62–6.8	3		575.287	32.3526
		6.81–8.48	4		795.247	44.7225
		8.49–12	5		82.754	4.6539

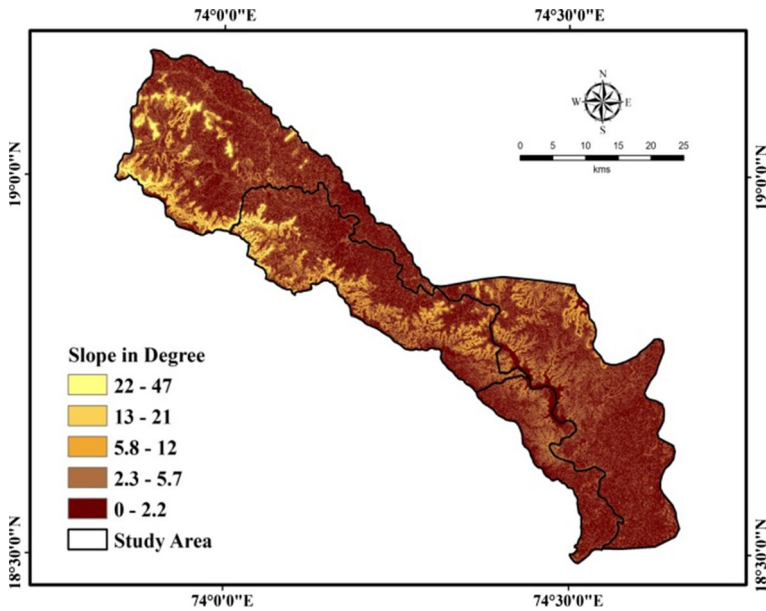


**Fig. 5** Land slope

and the hydraulic properties of the soil/rock material present in this zone play a significant role in supporting the green vegetative cover. The amount of water that clings the soil particles is very crucial during drought conditions; hence, it is imperative to measure the water/moisture content in this zone. After fulfilling the water requirement of vadose zone, i.e., when the field capacity stage is approached, the excess water starts draining with the gravity in the zone of saturation; hence, thicker vadose zone imparts delayed effect to the aquifer recharge. The vadose zone thickness varies from 0.84 to 7.46 m below ground level (bgl). The thickness of vadose zone reduces toward southeastern and central parts of the basin (Fig. 6).

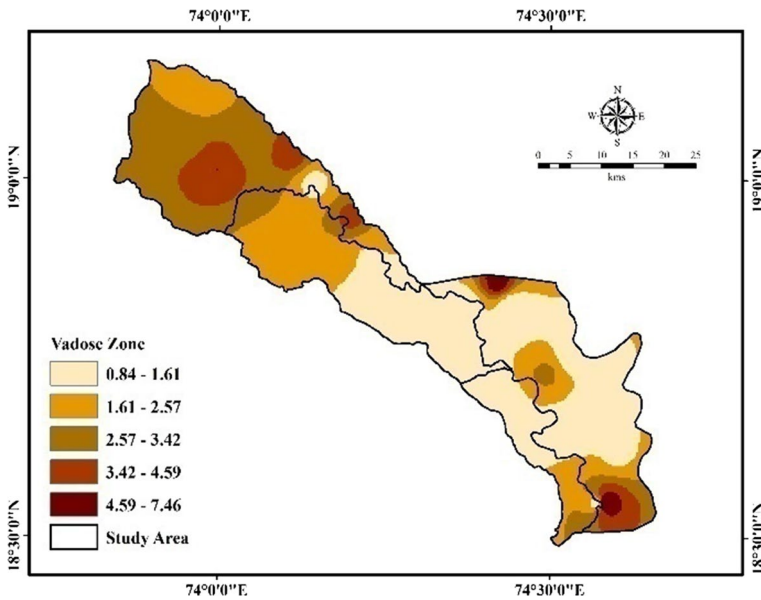


**Fig. 6** Thickness of vadose zone

#### 4.1.5 Soil depth

A well-defined soil horizon is developed at very few locations in the basin. The soil is reddish brown in color and exhibits mud cracks, which justifies the semiarid climate in the area. The soil wilting point is crucial in assessing the agricultural drought in a region. Due to urbanization and deforestation, the soil erosion rate is increasing especially in the NW part of the basin. The soil from the study area is sandy loam, sandy clay loam and loamy sand types, and it has been observed that the soil depth varies from 75 to 100 cm along the main river channel, valley, and valley fill regions. In the southern part of the study area, slightly deep (50 to 75 cm) soil layer is observed. Most of the area (61.69%, Table 3) shows very shallow to shallow depth of soil (< 10 cm) (Fig. 7). The moisture retaining capacity of soil facilitates the green cover and frequency of cultivation, and hence the highest ranks are allocated to the areas having poor or thin soil cover.

#### 4.1.6 Land-use/land-cover (LU/LC)

The land utilization type is a key factor in framing the hydrological setup of any river basin/watershed. The land use/land cover plays a fundamental role in drought severity mapping. The land cover generating more runoff contributes to scarcity of this precious resource. An object-based image analysis of upper Bhima catchment by Samal and Gedam (2012) revealed that there is a significant reduction in stream flow due to the urbanization, industrialization and conversion of wasteland into agriculture.

Agriculture, hills, barren land, fallow land, settlement, vegetation and water body are the land-use classes formulated to understand the land utilization pattern in the upper Bhima basin. Accuracy assessment analysis was conducted to check the correctness of land-use classes. The analysis revealed that 1080.801sq. km (59.78%) area has been covered by

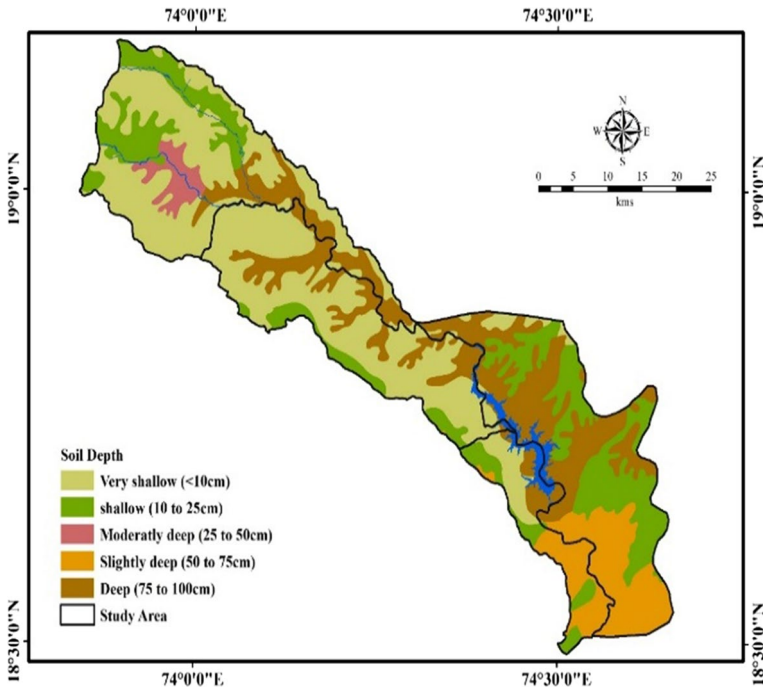


**Fig. 7** Soil depth

agriculture, whereas 500.510 sq. km (28.15%) by barren land and hills and 197.01 sq. km (11.07%) area is covered by other land-use types (Table 3 and Fig. 8). Agriculture is the major land-use type; hence, water demand for irrigation is high in the area. The surface water irrigation is prominent in command area covering southeast part of the basin. Forest, agriculture and water body categories have been assigned with the lowest ranks because of the least possibility of drought hazard.

#### 4.1.7 Water harvesting structures (WHS)

In hard rock terrain like basalt, due to poor permeability, the surface water conservation structures are highly recommended to cater the domestic and agricultural needs. The objective and type of these structures vary according to their placement in runoff, recharge or discharge zones in watershed. The ridge to valley conservation measures are common, and success stories have been reported from Maharashtra.

Continuous contour trenching (CCT), cement nala bunds (CNB), check dam and farm ponds (FP) were observed throughout the area wherein majority of the WH structures have been built on moderate to plain land (Fig. 9). Apart from this, in the lower part of the basin, major masonry dam has also been observed. Artificial recharge to aquifers in the area is possible due to these WHSs. As majority of the area is agricultural, farm ponds, stream bunds and check dams are built on large scale to cater the irrigational demand. These structures conserve the post-monsoonal river discharge and facilitate winter crops as well as summer crops in few areas. The density of WH structures is high toward SE region. The

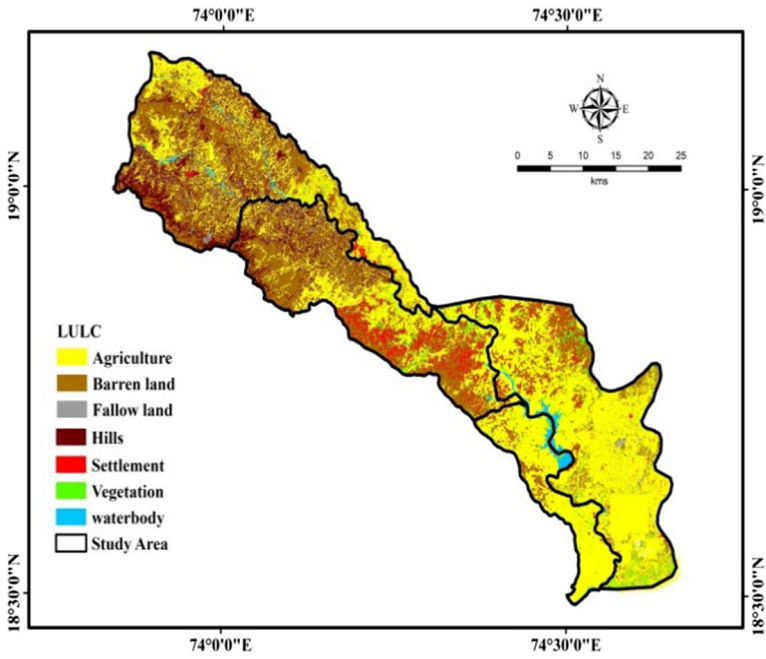


Fig. 8 LU/LC

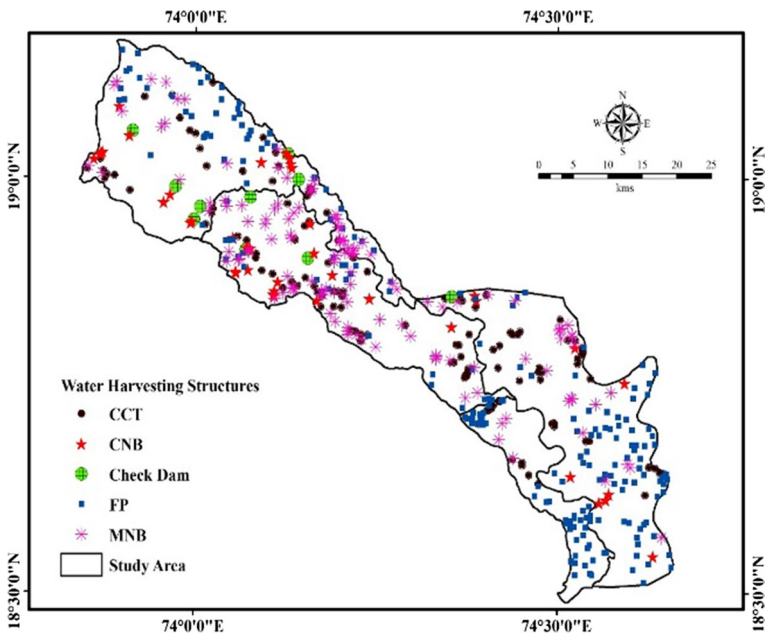


Fig. 9 Location of WHS

high density of WHS indicates ample availability of surface water and less possibility of water scarcity; therefore, minimum ranks are given to the areas with high WHS density.

### 4.1.8 Geomorphology

Majority of the area is a top plateau of the gigantic Deccan Volcanic Province (86.23%, Table 3). The other dominating morphology is of denudational hills and ridges, which occupy the northwestern part of the basin. The area exhibits various landform types, namely upper and middle plateau, alluvial plain, denudational hills and denudational slopes. Most of the study area is a part of upper and middle plateau (Fig. 10). The plateau area being gently sloping to flat, the surface runoff is moderate and thus availability of surface water is more as compared to hilly area.

### 4.1.9 Drainage density

The drainage density represents the total length of streams per unit area and expressed in km/sq. km. It is a sensitive parameter that, in many ways, links the landform attributes of the basin with the processes operating along stream course (Gregory and Welling 1973). It affects the rate of infiltration and surface discharge. A low drainage density indicates that most of the rainwater infiltrates in the subsurface and hence few channels are formed to carry the generated surface runoff (Rogers 1971). Drainage density reflects the relationship between erosive power of overland flow and the resistance of surface soils and rocks. Soil and rocks with a high infiltration rate reduce overland flow, and consequently drainage density is low in that region.

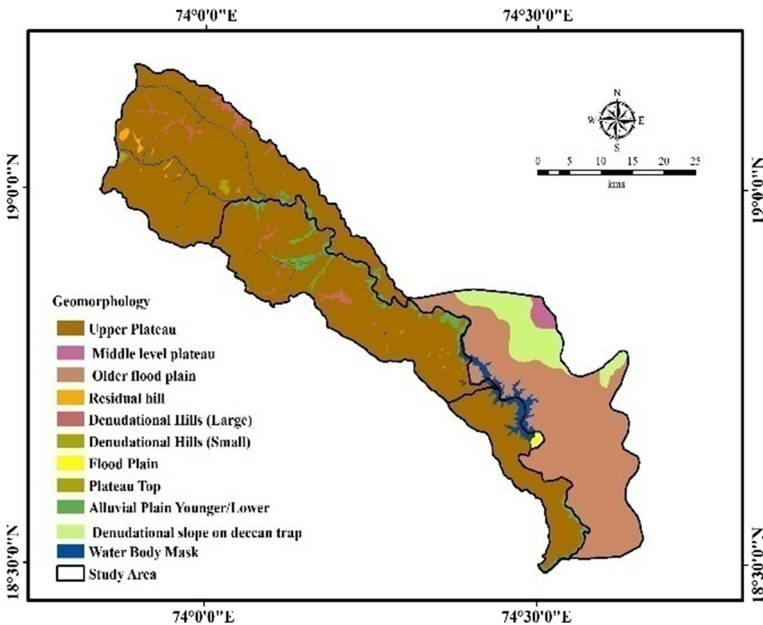


Fig. 10 Geomorphology

The higher drainage density results in more surface water flow in that area and hence prone to drought condition as seen in the northwestern hilly region of the basin. About 30% of the area experiences high drainage density (Table 3). Thus, higher drainage density has been observed in the upper peripheral part and low drainage density in the southern and southeastern parts of the area (Fig. 11). The highest ranks have been assigned to the areas showing the highest drainage density because of the less soil–water interaction and poor infiltration.

#### 4.1.10 Groundwater level fluctuation

The phreatic aquifers are mostly occurring up to the depth of 15 m in the basin. The weathered/fractured zone is underlain by hard massive basalts that act as a base rock of the phreatic aquifer, limiting its downward extent. The groundwater in these shallow aquifers gets replenished annually, and therefore, the status of water levels and its fluctuation play a key role in the assessment of drought. The groundwater levels in dug wells deplete due to several reasons, viz. rainfall variation, groundwater withdrawal during rainy season (prolong dry spell) for irrigating rain-fed crops, increase in the demand and due to the hydraulic connectivity with the deeper confined aquifers. Groundwater level fluctuation is directly proportional to drought severity. The average groundwater level fluctuation in the area ranges between 1.55 and 12 m (Fig. 12). High fluctuation (6–12 m) is observed in patches throughout the basin (highest ranks allocated) that mostly may be due to the unprecedented withdrawal for crop irrigation and domestic use.

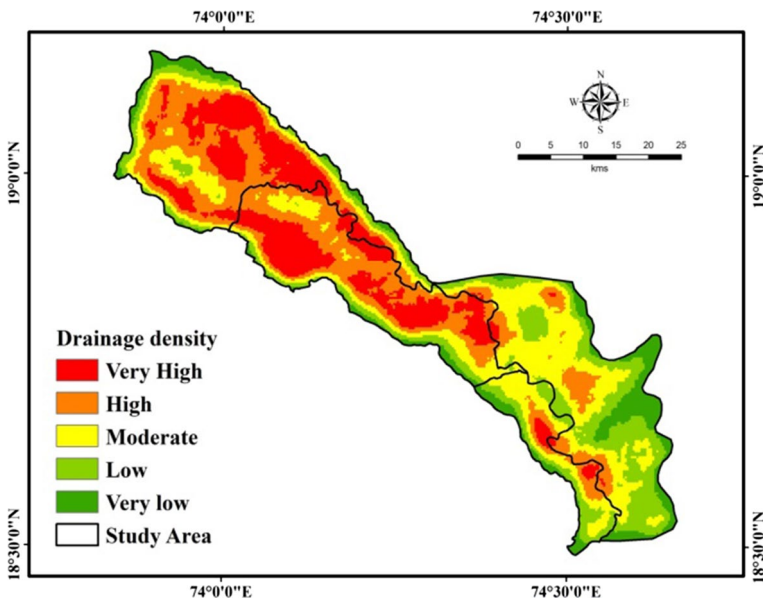


Fig. 11 Drainage density

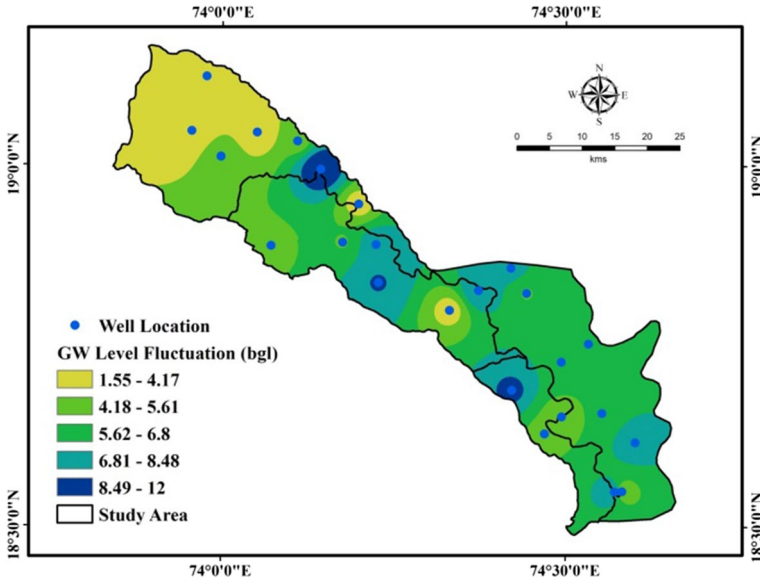


Fig. 12 GW level fluctuation

#### 4.1.11 Weight assignment using AHP

As the matrix is symmetrical, the lower half numbers are just the reciprocal of the values allocated to corresponding upper diagonal cells. The comparison matrix has been designed considering ten influencing factors contributing to drought severity (Table 4). Table 5 depicts the normalized pairwise comparison matrix.

Priority vector was computed by considering the comparison matrix and weighted score values. The product of weighted sum and score generated consistency measure values. Further, the average of consistency measure values was obtained to get the  $\lambda$  max (10.95). The closeness of  $\lambda$  max value to n (number of criteria) reflects the higher accuracy in judgment. The consistency index value obtained is 0.1060, and RI for the magnitude of 10 criteria is 1.49. The CR value computed for drought severity zonation mapping is 0.071188 depicting the consistency in weights assigned to various factors.

#### 4.1.12 Reclassification and integration of the thematic layers

GIS executes the database operations such as query building, attribute modification and statistical analysis. This makes GIS different from other information systems and elevating its utility among a wide range of public and private enterprises for explaining events, predicting scenarios and planning strategies (Subramani and Deepa 2016).

Reclassification of the thematic raster layers into five categories was performed by assigning ranks between 1 and 5 to each sub-feature class of the corresponding theme. During the reclassification, certain feature classes were merged to form a single class, e.g., in LU/LC map out of seven feature classes, two classes, namely water body and natural vegetation, were allotted with the same ranks and merged into a single class. Likewise, based on necessities the number of classes was reduced for other themes also.

**Table 4** Pairwise comparison matrix

Criteria	NDVI	Rainfall	Slope	VZ	SD	LULC	WHS	GM	Dd	GWF
NDVI	1	2	3	2	2	2	0.5	3	3	7
Rainfall	0.5	1	3	5	4	2	3	3	5	5
Slope	0.3333	0.3333	1	2	2	3	5	3	4	0.333
Vadose zone	0.5	0.2	0.5	1	3	2	0.5	3	4	5
Soil depth	0.5	0.25	0.5	0.3333	1	2	2	4	5	6
LULC	0.5	0.5	0.3333	0.5	0.5	1	0.3333	2	2	4
WHS	2	0.3333	0.2	2	0.5	3	1	2	3	2
Geomorphology	0.3333	0.3333	0.3333	0.3333	0.25	0.5	0.5	1	0.5	1
Dd	0.3333	0.2	0.25	0.25	0.2	0.5	0.3333	2	1	3
GW fluctuation	0.1428	0.2	3	0.2	0.1666	0.25	0.5	1	0.3333	1
Sum	6.14285	5.35	12.11667	13.6166	13.616	16.25	13.66667	24	27.83333	34.33333

**Table 5** Normalized pairwise comparison matrix

Criteria	NDVI	Rainfall	Slope	Vadose zone	Soil depth	LULC	WHS	Gm	Dd	GWF	Sum	Score
NDVI	0.162	0.373	0.247	0.146	0.146	0.123	0.036	0.125	0.107	0.203	1.674	0.1674
Rainfall	0.081	0.186	0.247	0.367	0.293	0.123	0.219	0.125	0.179	0.145	1.969	0.1969
Slope	0.054	0.062	0.082	0.146	0.146	0.184	0.365	0.125	0.143	0.009	1.321	0.1321
Vadose zone	0.081	0.037	0.041	0.073	0.220	0.123	0.036	0.125	0.143	0.145	1.027	0.1027
Soil depth	0.081	0.046	0.041	0.024	0.073	0.123	0.146	0.166	0.179	0.174	1.057	0.1057
LU/LC	0.081	0.093	0.027	0.036	0.036	0.061	0.024	0.083	0.071	0.116	0.633	0.0633
WHS	0.325	0.062	0.016	0.146	0.036	0.184	0.073	0.083	0.107	0.058	1.095	0.1095
Geomorphology	0.054	0.062	0.027	0.024	0.018	0.030	0.036	0.041	0.017	0.029	0.343	0.0343
Dd	0.054	0.037	0.020	0.018	0.014	0.030	0.024	0.083	0.035	0.087	0.407	0.0407
GW fluctuation	0.023	0.037	0.247	0.014	0.012	0.015	0.036	0.041	0.011	0.029	0.469	0.0469
CR = 0.071188											10	$\Sigma = 1$

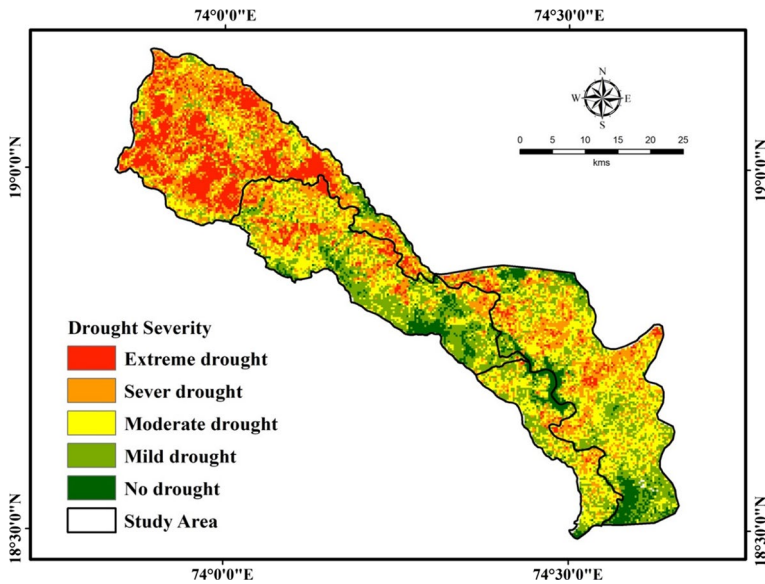


**Fig. 13** Drought severity zonation map

**Table 6** Drought severity classes with areal extent

Drought class	Area (km <sup>2</sup> )	Area (%)
Extreme drought	187.73	10.77
Severe drought	427.24	24.51
Moderate drought	547.03	31.38
Mild drought	429.80	24.65
No drought	151.52	08.69

The integration of thematic layers has been carried out by weighted overlay analysis, and the resultant map revealed the areas under variable degree of drought. This output map was further reclassified using natural breaks method to divide the area into extreme, severe, moderate, mild and no drought zones (Fig. 13). The zonation map exhibits about 187sq km area (about 11%) under extreme drought condition having hills, fallow and barren land as major land use, low to moderate soil depth with poor water holding capacity, steep slopes, poor density of WH structures, high drainage density indicating more surface runoff and moderate to high groundwater level fluctuation occupying majority of the northwestern part of the basin (Table 6).

While 427.24sq km (24.51%) area represents 'severe drought,' 547.03sq km (31.38%) area is covered under 'moderate drought' severity zone. In these zones, the larger area is under agriculture posing high demand of water with moderate density of water harvesting structures, built-up land, moderate thickness of vadose zone, moderate drainage density, low to moderate rainfall and high groundwater level fluctuation. Chinchni dam is constructed on Ghod river in the southeastern part of the study area, and canal irrigation supports the agricultural practices in nearby areas. Moreover, the dug wells are in

hydraulic connectivity with dam water; therefore, the region is under mild to no drought zone (Fig. 14).

### 4.1.13 Verification of drought severity model

The drought zonation map generated for the upper Bhima area has been validated by superimposing tanker-fed villages. High frequency of villages has been observed in extreme drought area followed by severe and moderate severity zones. The small habitations and hamlets situated in hilly terrain in the northwestern part of the study area face severe drinking water scarcity and depend on the tanker water supply, especially in severe summer months.

## 5 Conclusions and recommendations

Drought does not merely happen to be a natural phenomenon. It affects every climatic zone worldwide involving multiple sectors and hence draws the attention of researchers and planners to hazard mapping and risk assessment.

A study was conducted in parts of the upper Bhima river basin to explore the efficacy of integrated GIS and AHP techniques in drought hazard mapping. GIS helps in processing spatiotemporal data of large areas in short duration and explicitly executes the database operations such as query building and statistical analysis, whereas AHP facilitates

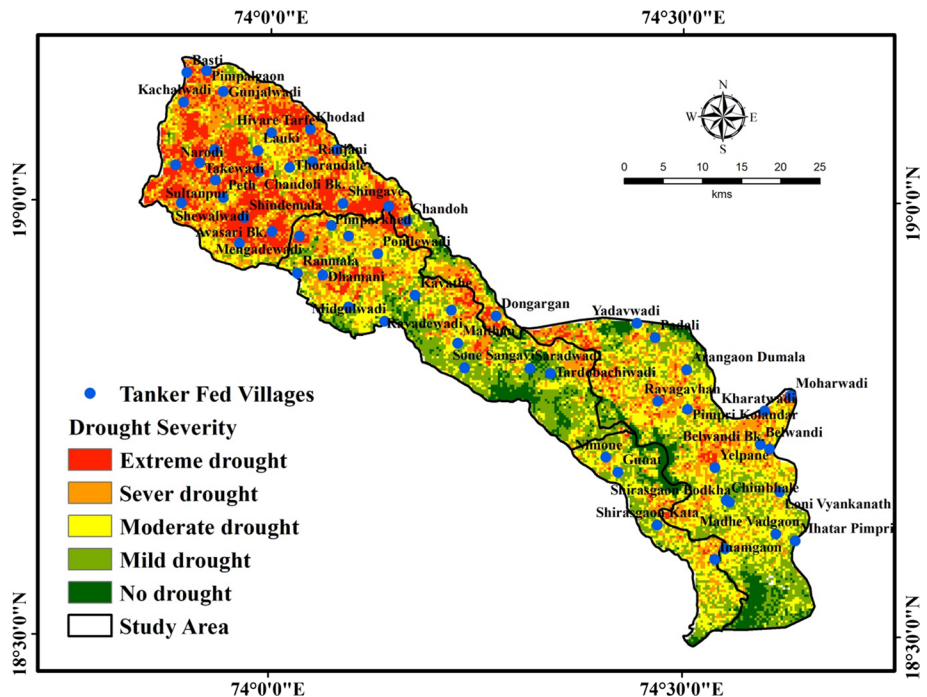


Fig. 14 Superimposition of tanker-fed villages on drought zonation map

the justifiable assignment of weights to influential parameters systematically with a reliable accuracy through pairwise comparison matrix to solve multi-criteria decision-making problems.

It has been found that the AHP is a powerful tool of normalization that removed the bias in weight allocation and efficiently established the hierarchical relationship among the factors affecting drought severity, viz. NDVI, rainfall, slope, vadose zone, soil depth, LULC, water harvesting structures, geomorphology, drainage density and groundwater level fluctuation, wherein GIS helped to combine these weighted thematic layers to produce drought zonation map.

The resultant map revealed that the zones with extreme, severe, moderate, mild and no drought cover 187.73, 427.24, 547.03, 429.80 and 151.52 sq. km area, respectively. The villages falling in extreme or severe drought zones experience drinking water scarcity taking a large toll on the government functionaries to provide water to suffice the drinking and domestic needs. These villages have to be provided with relief measures like piped water supply schemes, gravity-based water supply, spring water storage tanks, exploring perched aquifers, etc. The water budget exercise at village level is recommended to understand the water requirement for drinking as well as irrigation purposes and accordingly shift from cash crop to local suitable crop and less water-intensive crop to combat the scarcity.

The present study underlined the paucity of hydrogeological field data, especially in hilly and highly undulating basaltic terrain. There is a need of establishing a network of piezometers and digital water level recorders/sensors that would help in characterizing the heterogeneous basaltic aquifer. Besides, in light of climate variability the high frequency rainfall, temperature and evapotranspiration data are necessary to strengthen the predictability of drought. This study brings out avenues for future research to evaluate vulnerability involving relevant socioeconomic and ecological factors.

## References

- Chen YR, Yeh CH, Yu B (2011) Integrated application of the analytic hierarchy process and the geographic information system for flood risk assessment and flood plain management in Taiwan. *Nat Hazards* 59(3):1261–1276
- Chopra P (2006) Drought risk assessment using remote sensing <https://www.un-spider.org/node/7903> and GIS: A case study of Gujarat. Master thesis submitted to International Institute for Geo-Information Science and Earth Observation, ITC, Enschede, The Netherlands
- Dash SK, Kulkarni MA, Mohanty UC, Prasad K (2009) Changes in the characteristics of rain events in India. *J Geophys Res* 114:D10109
- Eslamian S (ed) (2014) Handbook of engineering hydrology: modeling, climate change, and variability. CRC Press, Boca Raton
- Gaur A, McCornick PG, Turrall H, Acharya S (2007) Implications of drought and water regulation in the Krishna Basin, India. *Int J Water Resour Dev* 23(4):583–594
- Golian S, Mazdiyasn O, AghaKouchak A (2015) Trends in meteorological and agricultural droughts in Iran. *Theoret Appl Climatol* 119:679–688
- Gregory KJ, Walling DE (1973) Drainage basin form and processes: a geomorphological approach. Halsted Press, New York, p 456
- Han P, Wang PX, Zhang SY, Zhu DH (2010) Drought forecasting based on the remote sensing data using ARIMA models. *Math Comp Model* 51:1398–1403
- Kamali B, Houshmand KD, Yang H, Abbaspour K (2017) Multilevel drought hazard assessment under climate change scenarios in semi-arid regions—A case study of the Karkheh river basin in Iran. *Water* 9(4):241
- Khaleghi S, Mahmoodi M (2017) Assessment of flood hazard zonation in a mountainous area based on GIS and analytical hierarchy process. *Carpathian J Earth Environ Sci* 12(1):311–322

- Liu C, Fu C, Shiu CJ, Chen JP, Wu F (2009) Temperature dependence of global precipitation extremes. *Geophys Res Lett* 36:L17702
- Malczewski J (1999) GIS and multicriteria decision analysis. Wiley, New York
- McKee TB, Doesken NJ, Kliest J (1993) The relationship of drought frequency and duration to time scales. In: Proceedings of the 8th conference on applied climatology, 17–22 January, Anaheim. American Meteorological Society: Boston 179–184
- Mishra A, Chen LS (2014) Changes in precipitation pattern and risk of drought over India in the context of global warming. *JGR Atmos* 119(13):7833–7841
- Murthy CS, Singh J, Kumar P, Sessa Sai MVR (2016) Meteorological drought analysis over India using analytical framework on CPC rainfall time series. *Nat Hazards* 81:573–587
- Palchaudhuri M, Biswas S (2016) Application of AHP with GIS in drought risk assessment for Puruliya district, India. *Nat Hazards* 84(3):1905–1920
- Palmer WC (1965) Meteorological drought. Research paper no. 45. U.S. Department of Commerce Weather Bureau, Washington, DC
- Palmer WC (1968) Keeping track of crop moisture conditions, nationwide: the new crop moisture index. *Weatherwise* 21:156–161
- Pandey S, Pandey AC, Nathawat MS, Kumar M, Mahanti NC (2012) Drought hazard assessment using geoinformatics over parts of Chotanagpur plateau region, Jharkhand, India *Nat Hazards* 63(2):279–303
- Pathak AA, Dodamani BM (2020) Trend analysis of rainfall, rainy days and drought: a case study of Ghataprabha River Basin. *India Model Earth Syst Environ* 6:1357–1372
- Pogarčić I., Frančić M., Davidović V (2008) Application of AHP method in traffic planning. In: 16th International Symposium on Electronics in traffic planning
- Prathumchai K, Honda K, Nualchawee K (2001) Drought risk evaluation using remote sensing and GIS: a case study in Lop Buri Province. In: 22nd Asian conference on remote sensing. Singapore
- Rogers WJ (1971) Hydrograph analysis and some related variables in quantitative geomorphology—Some aspect and applications. State University of New York, New York
- Saaty TL (1977) A scaling method for priorities in hierarchical structures. *J Math Psychol* 15(3):234–281
- Saaty TL (1980) The analytic hierarchy process. McGraw Hill international, New York, pp 1–287
- Saaty TL, Vargas LG (1991) Prediction, projection, and forecasting: Applications of the analytic hierarchy process in economics, finance, politics, games, and sports. Springer. ISBN 978-94-015-7954-4
- Impact of land use dynamics on stream flow: a case study in upper Bhima basin, Maharashtra, India. In: IEEE International Geoscience and Remote Sensing Symposium, Munich, pp. 7165–7168
- Sheffield J, Wood EF (2012) Drought: past problems and future scenarios. Taylor and Francis. ISBN: 9781849710824
- Stefanidis S, Stathis D (2013) Assessment of flood hazard based on natural and anthropogenic factors using analytic hierarchy process (AHP). *Nat Hazards* 68(2):569–585
- Subramani T, Deepa CM (2016) Study and analysis of water level fluctuation by using GIS in Tiruppur District. *Int J Emerg Trend Technol Comp Sci* 5(3):159–170
- Sun YS, Solomon A, Dai R, Portmann RW (2007) How often will it rain? *Jour Clim* 20:4801–4818
- Svoboda M, LeComte D, Hayes M, Heim R, Gleason K, Angel J, Miskus D (2002) The drought monitor. *Bull Am Meteor Soc* 83(8):1181–1190
- Tao J, Zhongfa Z, Shui C (2011) Drought monitoring and analyzing on typical karst ecological fragile area based on GIS. *Proc Environ Sci* 10:2091–2096
- Thomas T, Jaiswal RK, Galkate R, Nayak PC, Ghosh NC (2016) Drought indicators-based integrated assessment of drought vulnerability: a case study of Bundelkhand droughts in central India. *Nat Hazards* 81(3):1627–1652. <https://doi.org/10.1007/s11069-016-2149-8>
- Van Loon AF, Stahl K, Di Baldassarre G, Clark J, Rangelcrot S, Wanders N, Gleeson T, Van Dijk AIJM, Tallaksen LM, Hannaford J, Uijlenhoet R, Teuling AJ, Hannah DM, Sheffield J, Svoboda M, Verbeiren B, Wagener T, Van Lanen HAJ (2016) Drought in a human-modified world: Reframing drought definitions, understanding, and analysis approaches. *Hydrol Earth Syst Sci* 20:3631–3650
- Vicente-Serrano SM, Beguería S, López-Moreno JI (2010) A multiscale drought index sensitive to global warming: the standardized precipitation evapotranspiration index. *J Clim* 23:1696–1718
- Vijaya Kumar P, Osman M, Mishra PK (2019) Development and application of a new drought severity index for categorizing drought-prone areas: a case study of undivided Andhra Pradesh state, India. *Nat Hazards* 97:793–812
- Yihdego Y (2017) Drought and pest management. In: Eslamian S (ed) Handbook of drought and water scarcity. CRC Press, Boca Raton, pp 279–292
- Yihdego Y, Vaheddoost B, Al-Weshah RA (2019) Drought indices and indicators revisited. *J Arab J Geosci* 12(3):69

Zagade N, Kadam AK, Umrikar BN, Maggirwar BC (2018) Remote sensing-based assessment of agricultural droughts in sub-watersheds of upper Bhima basin. *India J Remote Sens Land* 2(2):105–111

**Publisher's Note** Springer Nature remains neutral with regard to jurisdictional claims in published maps and institutional affiliations.